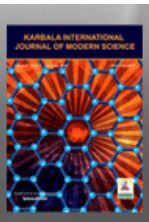

Karbala International Journal of Modern Science

Volume 9 | Issue 3 Article 11

# Representing quantum spins in different coordinate systems for modelling rigid body orientation

Nadjet Zioui
*Département de Génie Mécanique, Université du Québec à Trois-Rivières, 3351 Boulevard des Forges, Trois-Rivières, QC G8Z 4M3, Canada*, nadjet.zioui@uqtr.ca

Aicha Mahmoudi
*(Projet Véo, Université de Sherbrooke, 2500 Bd de l'Université, Sherbrooke, QC J1K 2R1*

Mohamed Tadjine
*LCP (Laboratoire de Commande des Processus), École Nationale Polytechnique d'Alger, c 10 Rue des Frères OUDEK, El Harrach 16200, Algeria*

# Representing quantum spins in different coordinate systems for modelling rigid body orientation


## Abstract

Various methods for representing the spatial orientation and rotation of objects are presented and compared with the quantum bit state representation. By contrasting spherical, Euler angle, quaternion, and quantum spin coordinate systems, this work highlights important concepts regarding the rotation axis of the X gate. Several ambiguities and incomplete definitions associated with the qubit state representation are discussed, such as the spin around the qubit itself and the explanation of the considered rotation angles and signs. A mathematical analysis of the physical meaning of each eigenstate is provided along with a new comprehensive and meaningful YPR-based 3D representation of a qubit state.



## Keywords

Qubit state; Quantum spins; 3D rotations; Spherical coordinates; Yaw, pitch, and roll angles; Quaternions.

RESEARCH PAPER

# Representing Quantum Spins in Different Coordinate Systems for Modelling Rigid Body Orientation

Nadjet Zioui [a,*], Aicha Mahmoudi [b], Mohamed Tadjine [c]

[a] Département de Génie Mécanique, Université du Québec à Trois-Rivières, 3351 Boulevard des Forges, Trois-Rivières, QC G8Z 4M3, Canada
[b] Projet Véo, Université de Sherbrooke, 2500 Bd de l'Université, Sherbrooke, QC J1K 2R1, Canada
[c] LCP (Laboratoire de Commande des Processus), École Nationale Polytechnique d'Alger, c 10 Rue des Frères OUDEK, El Harrach, 16200, Algeria

**Abstract**

**Various methods for representing the spatial orientation and rotation of objects are presented and compared with the quantum bit state representation. By contrasting spherical, Euler angle, quaternion, and quantum spin coordinate systems, this work highlights important concepts regarding the rotation axis of the X gate. Several ambiguities and incomplete definitions associated with the qubit state representation are discussed, such as the spin around the qubit itself and the explanation of the considered rotation angles and signs. A mathematical analysis of the physical meaning of each eigenstate is provided along with a new comprehensive and meaningful YPR-based 3D representation of a qubit state.**

*Keywords:* Qubit state, Quantum spins, 3D rotations, Spherical coordinates, Yaw, pitch, and roll angles, Quaternions

## 1. Introduction

Computing the orientation of rigid bodies is an important task in many fields of engineering, including robotics and aeronautics. Specifically in robotics, orientation plays a fundamental role in numerous industrial, medical, and surgical applications.

Various methods are commonly used to model and represent the orientation of a rigid body, such as the spherical coordinates and the Euler angles, or the yaw, pitch, and roll (YPR) angles. These methods use $3 \times 3$ matrices to hold the projection coordinates of the three unit vectors, which makes them memory- and resource-intensive. In contrast, compact methods have also been developed, such as quaternions and dual quaternions. This representation uses only four components: one real and three imaginary parts. All the above methods have been successfully used in multiple applications; however, they are all designed for classical computers.

With the advent of quantum computers, new challenges arise concerning the modelling and control of rigid body orientation using quantum tools, as well as establishing bridges between classical and quantum methods. Quantum computing is expected to vastly outperform conventional computers. Thus, quantum computing methods have been developed and implemented in various fields and applications [1−6]. For example, qubit states have been used to model the position and orientation of an industrial robotic arm end effector using the equivalence between the Pauli gates and quaternions [7]. A method of defining the end effector orientation using a single qubit state based on the elementary rotation gates is more efficient compared with the results obtained using YPR angles based on a homogenous matrix [8]. Moreover, a quantum forward kinematics model has been introduced for an industrial robotic arm, in which a

Received 11 March 2023; revised 6 July 2023; accepted 8 July 2023.
Available online 8 August 2023

* Corresponding author.
E-mail address: nadjet.zioui@uqtr.ca (N. Zioui).

https://doi.org/10.33640/2405-609X.3313

systematic formulation of the D-H matrix is presented using a single qubit state [9]. Owing to the complexity of the quantum representation using only two components to express a qubit state, especially compared with the intuitive representation in three-dimensional (3D) vector space, the real-world meaning of this new formalism remains somewhat obscure. We have found no published validation of each eigenstate in terms of quantum computing basics.

In the present study, we focus on the fundamental quantum spins, or rotations, to compare the spherical, Euler angle, and quaternion orientation representations, to help clarify the true physical meaning of the quantum states in the intuitive 3D space.

The proposed work highlights three significant concerns and suggests potential solutions: first, the lack of information in the current Bloch representation of a qubit state in relation to the self-spin angle (around the oz axis); second, the basic specifications of the axes in 3D space that do not correspond to the existing representation; and third, the ratio of the oy axis rotation angle must be considered, not only for sandwich products but also to indicate the genuine rotation angles in real-world 3D space.

The findings of this work may help to establish quantum versions of several conventional computing concepts and thus provide a starting point for a variety of real-world applications that require appropriate and optimal orientation models, such as quadrotors, quadcopters, UAVs, and UGVs [10–14], mobile robots, and robotic manipulators [15].

## 2. Materials and methods

### 2.1. The qubit and quantum operators

A qubit is the basic element of information in quantum computing. Whereas a conventional bit has two possible values (0 or 1), a qubit state has infinite possible values that can each be expressed as a linear combination of the two eigenstates 0 and 1, denoted by $|0\rangle$ and $|1\rangle$, respectively, as represented in equation (1) [16–18].

$$|q\rangle = \alpha|0\rangle + \beta|1\rangle \tag{1}$$

Where $\alpha$ and $\beta$ are the projections of the qubit state $|q\rangle$ on the eigenstates $|0\rangle$ and $|1\rangle$, respectively. They are complex numbers, such that $|\alpha|^2 + |\beta|^2 = 1$, and can be expressed as follows:

$$\begin{cases} \alpha = Re_{|0\rangle} + iIm_{|0\rangle} \\ \beta = Re_{|1\rangle} + iIm_{|1\rangle} \end{cases} \tag{2}$$

Where $Re_{|0\rangle}$ and $Im_{|0\rangle}$ are the real and imaginary components of $\alpha$, $Re_{|1\rangle}$ and $Im_{|1\rangle}$ are the real and imaginary components of $\beta$, and $i$ is a purely imaginary number, such that $i^2 = -1$. The eigenstates $|0\rangle$ and $|1\rangle$ are usually represented in the two-dimensional (2D) vector space as $|0\rangle = \begin{pmatrix} 1 \\ 0 \end{pmatrix}$ and $|1\rangle = \begin{pmatrix} 0 \\ 1 \end{pmatrix}$.

A single qubit state is usually represented in the 3D space using the Bloch sphere, as illustrated in Fig. 1, which corresponds to the mathematical expression of equation (3) [19,20].

$$|q\rangle = cos\frac{\theta}{2}|0\rangle + sin\frac{\theta}{2}e^{i\varphi}|1\rangle = \begin{pmatrix} cos\frac{\theta}{2} \\ sin\frac{\theta}{2}e^{i\varphi} \end{pmatrix} \tag{3}$$

Several operators exist, called quantum operators, which can alter a qubit's state. Quantum operators or gates can be expressed using four basic Hermitian matrices, known as the Pauli matrices (i.e., $\sigma_0$, $\sigma_x$, $\sigma_y$, and $\sigma_z$), as defined in expressions (4) through (7) [21].

$$\sigma_0 = \begin{pmatrix} 1 & 0 \\ 0 & 1 \end{pmatrix} \tag{4}$$

$$\sigma_x = \begin{pmatrix} 0 & 1 \\ 1 & 0 \end{pmatrix} \tag{5}$$

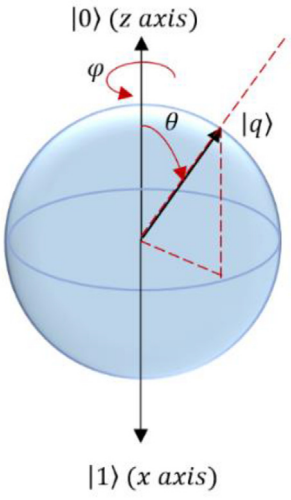


*Fig. 1. The Bloch sphere representation of a single qubit state.*

$$\sigma_y = \begin{pmatrix} 0 & -i \\ i & 0 \end{pmatrix} \tag{6}$$

$$\sigma_z = \begin{pmatrix} 1 & 0 \\ 0 & -1 \end{pmatrix} \tag{7}$$

The Pauli matrices, $\sigma_x$, $\sigma_y$, $\sigma_z$, and $\sigma_0$, are also known as the X, Y, Z, and identity gates, respectively. Any quantum operator can be expressed in terms of the Pauli gates, including the basic spins $R_x(\psi)$, $R_y(\theta)$, and $R_z(\varphi)$, or their respective rotations $\psi$, $\theta$, and $\varphi$ around the axes ox, oy, and oz, as shown in equation (8) through (10) [8].

$$R_x(\psi) = cos\frac{\psi}{2}\sigma_0 - i\sigma_x\, sin\frac{\psi}{2} = \begin{pmatrix} C\frac{\psi}{2} & -iS\frac{\psi}{2} \\ -iS\frac{\psi}{2} & C\frac{\psi}{2} \end{pmatrix} \tag{8}$$

$$R_y(\theta) = cos\frac{\theta}{2}\sigma_0 - i\sigma_y\, sin\frac{\theta}{2} = \begin{pmatrix} C\frac{\theta}{2} & -S\frac{\theta}{2} \\ S\frac{\theta}{2} & C\frac{\theta}{2} \end{pmatrix} \tag{9}$$

$$R_z(\varphi) = cos\frac{\varphi}{2}\sigma_0 - i\sigma_z\, sin\frac{\varphi}{2} = \begin{pmatrix} e^{-i\frac{\varphi}{2}} & 0 \\ 0 & e^{i\frac{\varphi}{2}} \end{pmatrix} \tag{10}$$

Where $C\theta$ and $S\theta$ are the cosine and sine of the angle $\theta$.

### 2.2. The spherical coordinates

Spherical coordinates allow for the representation of a vector in the 3D space using two angles, $\theta$ and $\varphi$, as illustrated in Fig. 2. A matrix transformation is defined to express the unit vectors $u_\rho$ and $u_\theta$, as expressed in relationship (11) [22,23].

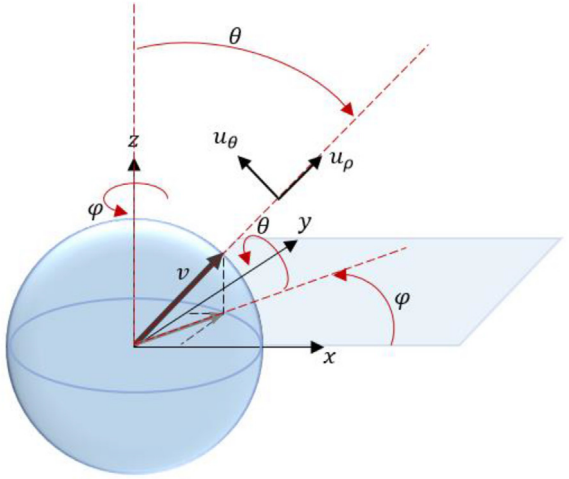


*Fig. 2. Spherical coordinate representation of a vector in 3D space.*

$$M_{sph}(\theta,\varphi) = \begin{pmatrix} S\theta C\varphi & C\theta C\varphi & -S\varphi \\ S\theta S\varphi & C\theta S\varphi & C\varphi \\ C\theta & -S\theta & 0 \end{pmatrix} \tag{11}$$

The first column of the matrix $M(\theta,\varphi)$ holds the coordinates of the unit vector denoted by $u_\rho$, and the second column holds the coordinates of unit vector $u_\theta$. Only two unit vectors are used in the spherical representation. The third unit vector contained in the matrix is denoted by $u_\varphi$. This last unit vector is obtained using the right-hand rule to complete the 3D orthonormal frame. This matrix should be expressed as the product of two elementary rotations, around the oz and oy axes, as shown in relationship (12). However, matrix $R'_{y3D}(\theta) = \begin{pmatrix} S\theta & C\theta & 0 \\ 0 & 1 & 1 \\ C\theta & -S\theta & 0 \end{pmatrix}$ is used instead of $R_{y3D}(\theta)$.

$$M_{sph}(\theta,\varphi) = R_{z3D}(\varphi)R_{y3D}(\theta) \tag{12}$$

Where $R_{z3D}(\varphi) = \begin{pmatrix} C\varphi & -S\varphi & 0 \\ S\varphi & C\varphi & 0 \\ 0 & 0 & 1 \end{pmatrix}$ and $R_{y3D}(\theta) = \begin{pmatrix} C\theta & 0 & S\theta \\ 0 & 1 & 0 \\ -S\theta & 0 & C\theta \end{pmatrix}$ are the elementary rotation matrices expressed in 3D space.

### 2.3. The yaw, pitch, and roll (YPR) angles

YPR angles provide another way to represent a vector in the 3D space. Widely used in robotics and aerospace engineering to model the orientation of rigid bodies, these three angles represent the body's orientation using three elementary rotations $R_{x3D}(\psi)$, $R_{y3D}(\theta)$, and $R_{z3D}(\varphi)$ around the ox, oy, and oz axes, respectively, as illustrated in Fig. 3. The resulting transformation matrix is provided in expression (13) [24].

$$M_{YPR}(\psi,\theta,\varphi) = R_{z3D}(\varphi)R_{y3D}(\theta)R_{x3D}(\psi) = \begin{pmatrix} C\theta C\varphi & S\psi S\theta C\varphi - C\psi S\varphi & C\psi S\theta C\varphi + S\psi S\varphi \\ C\theta S\varphi & S\psi S\theta S\varphi + C\psi C\varphi & C\psi S\theta S\varphi - S\psi C\varphi \\ -S\theta & S\psi C\theta & C\psi C\theta \end{pmatrix} \tag{13}$$

Where $R_{x3D}(\psi) = \begin{pmatrix} 1 & 0 & 0 \\ 0 & C\psi & -S\psi \\ 0 & S\psi & C\psi \end{pmatrix}$.

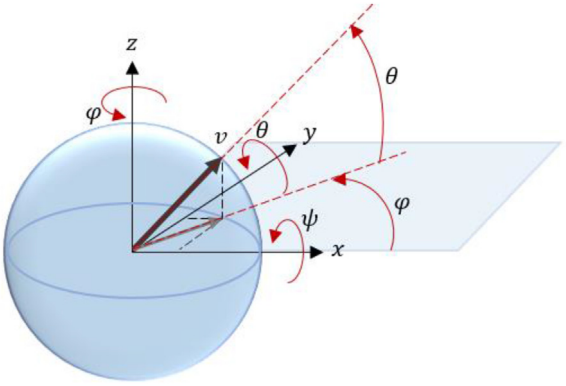


*Fig. 3. YPR representation of a vector in 3D space.*

### 2.4. The quaternions

Quaternions are hyper-complex numbers with one real and three imaginary components. A typical quaternion $q$ can be expressed by equation (14) [25,26].

$$q = r + xi + yj + zk \tag{14}$$

Where $r$ is the real component, $x$, $y$, and $z$ are the imaginary components, and $i$, $j$, and $k$ are the three purely imaginary numbers, such that $i^2 = j^2 = k^2 = -1$ and $ij = k$, $jk = i$, and $ki = j$. Quaternions can be used to describe the translation or rotation of a rigid body and have been extensively used in the kinematic modelling of robotics [27–33]. Equation (15) defines the translation, and relations (16) express the three elementary rotations $\psi$, $\theta$, and $\varphi$, around the three axes ox, oy, and oz, respectively [8,9].

$$q = xi + yj + zk \tag{15}$$

$$\begin{cases} q_x(\psi) = cos\dfrac{\psi}{2} + i\, sin\dfrac{\psi}{2} \\ q_y(\theta) = cos\dfrac{\theta}{2} + j\, sin\dfrac{\theta}{2} \\ q_z(\varphi) = cos\dfrac{\varphi}{2} + k\, sin\dfrac{\varphi}{2} \end{cases} \tag{16}$$

### 2.5. Methodology

The parallels between the above methods are described below to help clarify how the quantum spins method can achieve the same result. The various transform equivalences developed in each subsection are summarised in Fig. 4.

#### 2.5.1. From the spherical to the YPR coordinates

An intuitive way of finding the equivalence between the spherical and YPR representations is to set the angle $\psi$ to 0, which leads to relation (17).

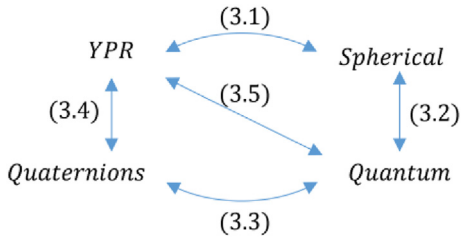


*Fig. 4. The equivalences between the methods used in this article to represent rigid body spatial orientation and trajectory.*

$$M_{YPR}(\psi = 0, \theta, \varphi) =$$

$$R_{z3D}(\varphi = 0) R_{y3D}(\theta) R_{x3D}(\psi) = \begin{pmatrix} C\theta C\varphi & -S\varphi & S\theta C\varphi \\ C\theta S\varphi & C\varphi & S\theta S\varphi \\ -S\theta & 0 & C\theta \end{pmatrix} \tag{17}$$

The obtained matrix is the result of a permutation between the columns of the matrix in relationship (11). A transformation matrix $M_{S-Y}$ (or $M_{Y-S}$) is necessary to switch from one representation to the other, as follows:

$$M_{YPR}(\psi = 0, \theta, \varphi) = M_{SPH}(\theta, \varphi)\, M_{S-Y} \tag{18}$$

$$M_{SPH}(\theta, \varphi) = M_{YPR}(\psi = 0, \theta, \varphi)\, M_{Y-S} \tag{19}$$

Where $M_{S-Y} = \begin{pmatrix} 0 & 0 & 1 \\ 1 & 0 & 0 \\ 0 & 1 & 0 \end{pmatrix}$ and $M_{Y-S} = {M_{S-Y}}^{-1} = \begin{pmatrix} 0 & 1 & 0 \\ 0 & 0 & 1 \\ 1 & 0 & 0 \end{pmatrix}$.

Relationships (18) and (19) state that the ox axis in the YPR representation is equivalent to the oy axis from the spherical representation, and the YPR representation's oy and oz axes are equivalent to the spherical representation's oz and ox axes, respectively, with the yaw angle considered to be 0.

#### 2.5.2. The qubit-to-spherical representation*

The principal source of inspiration for the Bloch sphere and the qubit state in equation (3) is the spherical coordinate system with angle half-values, whereby the oz axis is considered to be the qubit eigenvector $|0\rangle$, or eigenstate, and the unit vector $u_\rho$ is obtained as the result of applying the elementary rotations to this axis. The equivalences between the spherical and quantum expressions of a qubit state are illustrated in Fig. 5.

* Special description of the title (dispensable).

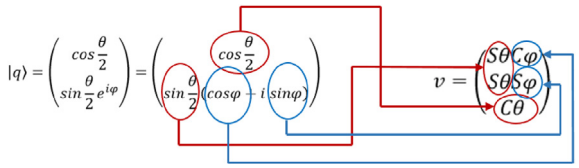

*Fig. 5. The equivalence between the quantum and spherical representations of the basic rotations.*

In the current quantum computing formalism, or Bloch sphere representation, eigenstate $|1\rangle$ is considered to be on the opposite side of the oz axis and hence linearly dependent on eigenstate $|0\rangle$, which leads to ambiguity because the two eigenstates are supposed to form the basis of a linear independence. One solution to this might be to consider half the rotation angles in relations (8) to (10), where the angle $\theta$ is divided by 2 and ranges from 0 to $\pi$ instead of 0 to $2\pi$. This results in an equivalent representation of the spherical coordinates and mathematically brings the eigenstate $|1\rangle$ to the right plane (ox, oy). However, this introduces ambiguity for the two remaining rotation angles because they must range from 0 to $2\pi$.

Finally, the qubit, as represented in the Bloch sphere and formulated in equation (3), does not consider the rotation of a qubit state around itself, and thus the equation is missing the third fundamental rotation $\psi$. Therefore, the eigenvector representation and the basic rotations in quantum computing need to be reformulated in greater detail.

### 2.5.3. The qubit-to-quaternion transformation

As quaternions have been widely used to model the rigid body's position and orientation, a useful first step towards a more coherent quantum representation of the possible qubit states is defining an equivalence and transformation from qubit states to quaternions. This qubit-to-quaternion transformation requires the equivalence to be established first between the Pauli matrices and the quaternions.

Expression (20) shows the representation of a given quaternion $q = r + x\,i + y\,j + z\,k$ in the 2D vector space [7]. Since a quaternion can be used to express the result of an operation, or an operator, expressing a quaternion using the Pauli matrices reveals its relationship to a qubit state and thus constitutes a first step towards a quantum transformation.

$$q = \begin{pmatrix} r+ix & y+iz \\ -y+iz & r-ix \end{pmatrix}$$

$$= r\begin{pmatrix} 1 & 0 \\ 0 & 1 \end{pmatrix} + i\,x\begin{pmatrix} 1 & 0 \\ 0 & -1 \end{pmatrix} - i\,y\begin{pmatrix} 0 & -i \\ i & 0 \end{pmatrix} + i\,z\begin{pmatrix} 0 & 1 \\ 1 & 0 \end{pmatrix}$$

$$= r\sigma_0 + i\,x\sigma_z - i\,y\sigma_y + i\,z\sigma_x \tag{20}$$

Relationship (20) states that for a given operator, the quantum and quaternion representations share a common real component and one of the imaginary components, which is equivalent to the oy axis projection. However, the ox axis component of a quaternion appears to correspond to the Pauli z component, and the z component corresponds to the x component, both with negative signs. Applying this quaternion operator to the oz axis unit vector $u_z = (0 \quad 0 \quad 0 \quad 1)^T$ or $\begin{pmatrix} 0 & i \\ i & 0 \end{pmatrix}$ leads to quaternion $q_z = (-z \quad y \quad -x \quad r)^T$:

$$q\,u_z = \begin{pmatrix} r+ix & y+iz \\ -y+iz & r-ix \end{pmatrix}\begin{pmatrix} 0 & i \\ i & 0 \end{pmatrix} = \begin{pmatrix} -z+iy & -x+ir \\ x+ir & -z-iy \end{pmatrix} \tag{21}$$

To fully clarify the relationship between the two representations, relationship (20) is rewritten in terms of the basic rotations, considering relations (16), such that the basic rotation matrices result in equations (22)–(24). These can be compared with their equivalent basic rotations expressed in the quantum formulation in equations (8)–(10).

$$q_x = cos\frac{\psi}{2}\sigma_0 + i\,\frac{\psi}{2}\sigma_z \tag{22}$$

$$q_y = cos\frac{\theta}{2}\sigma_0 - isin\frac{\theta}{2}\sigma_y \tag{23}$$

$$q_z = cos\frac{\varphi}{2}\sigma_0 + i\,sin\frac{\varphi}{2}\sigma_x \tag{24}$$

At a glance, these three equations imply the following:

The oz axis, which is considered the reference axis in the quantum formulation, appears to be equivalent to the ox axis in the quaternion representation, and the rotation angle around the qubit's oz axis is equivalent to the quaternion's $-\psi$ angle.

The oy axis appears to be the same in both representations.

The qubit's ox axis appears to be equivalent to the quaternion's oz axis, and the rotation angle around the qubit's ox axis is equivalent to the quaternion's $-\varphi$ angle.

In other words, to obtain the same operator matrix result in quantum computing as that obtained in quaternions, the operator $R_x(-\varphi)R_y(\theta)R_z(-\psi)$ should be used rather than $R_z(\varphi)R_y(\theta)R_x(\psi)$. Similarly, switching from the qubit representation to the quaternions implies the use of the transform $R_z(-\psi)R_y(\theta)R_x(-\varphi)$.

*2.5.4. The quaternions-to-YPR transformation*

There are several ways of transposing quaternions into YPR angles for representing orientations [34,35]. The following relationships can be used to go from YRP to quaternions (25) and from quaternions to YPR (26) [34].

$$\begin{cases} r = C\frac{\psi}{2}C\frac{\theta}{2}C\frac{\phi}{2} + S\frac{\psi}{2}S\frac{\theta}{2}S\frac{\phi}{2} \\ x = -C\frac{\psi}{2}S\frac{\theta}{2}S\frac{\phi}{2} + S\frac{\psi}{2}C\frac{\theta}{2}C\frac{\phi}{2} \\ y = C\frac{\psi}{2}S\frac{\theta}{2}C\frac{\phi}{2} + S\frac{\psi}{2}C\frac{\theta}{2}S\frac{\phi}{2} \\ z = -S\frac{\psi}{2}S\frac{\theta}{2}C\frac{\phi}{2} + C\frac{\psi}{2}C\frac{\theta}{2}S\frac{\phi}{2} \end{cases} \tag{25}$$

$$\begin{cases} \psi = \frac{1}{2}Asin(2(ry - zx)) \\ \theta = \frac{1}{2}Atan\,2\left(2(rx + yz), 1 - 2\left(x^2 + y^2\right)\right) \\ \varphi = \frac{1}{2}Atan\,2\left(2(rz + xy), 1 - 2\left(y^2 + z^2\right)\right) \end{cases} \tag{26}$$

The corresponding homogenous matrix can then be deduced as follows:

$$M_{YPR}(\psi,\theta,\varphi) = R_{z3D}(\varphi)R_{y3D}(\theta)R_{x3D}(\psi)$$

$$= \begin{pmatrix} r^2 + x^2 - y^2 - z^2 & 2xy - 2rz & 2ry + 2xz \\ 2rz + 2xy & r^2 - x^2 + y^2 - z^2 & 2yz - 2rx \\ 2xz - 2ry & 2rx + 2yz & r^2 - x^2 - y^2 + z^2 \end{pmatrix} \tag{27}$$

*2.5.5. The qubit-to-YPR transformation*

The equivalence between the qubit state and the YPR angles can be established using the three elementary rotation transformations in both representations, as well as the equivalence between the quaternions and the YPR angles, as shown above (subsection 3.3).

In 3D vector space, the matrix (13) defines the transformation resulting from applying the $\phi$, $\theta$, and $\psi$ basic rotations around the oz, oy, and ox axes, respectively. Similarly, in quantum computing, the application of the three elementary rotations $R_z(\phi)$, $R_y(\theta)$, and $R_x(\psi)$ results in the following operator:

$$R_z(\phi)R_y(\theta)R_x(\psi) = \begin{pmatrix} \left(C\frac{\psi}{2}C\frac{\theta}{2} + iS\frac{\psi}{2}S\frac{\theta}{2}\right)e^{-i\frac{\phi}{2}} & -\left(C\frac{\psi}{2}S\frac{\theta}{2} + iS\frac{\psi}{2}C\frac{\theta}{2}\right)e^{-i\frac{\phi}{2}} \\ \left(C\frac{\psi}{2}S\frac{\theta}{2} - iS\frac{\psi}{2}C\frac{\theta}{2}\right)e^{i\frac{\phi}{2}} & \left(C\frac{\psi}{2}C\frac{\theta}{2} - iS\frac{\psi}{2}S\frac{\theta}{2}\right)e^{i\frac{\phi}{2}} \end{pmatrix} \tag{28}$$

Applying the rotation operator (28) to the initial qubit state $|0\rangle$ results in the qubit state $|q\rangle$, defined as follows:

$$|q\rangle = R_z(\phi)R_y(\theta)R_x(\psi)|0\rangle = \begin{pmatrix} \left(C\frac{\psi}{2}C\frac{\theta}{2} + iS\frac{\psi}{2}S\frac{\theta}{2}\right)e^{-i\frac{\phi}{2}} \\ \left(C\frac{\psi}{2}S\frac{\theta}{2} - iS\frac{\psi}{2}C\frac{\theta}{2}\right)e^{i\frac{\phi}{2}} \end{pmatrix} \tag{29}$$

The components of a qubit state are expressed in greater detail as follows:

$$\begin{cases} Re_{|0\rangle} = C\frac{\psi}{2}C\frac{\theta}{2}C\frac{\phi}{2} + S\frac{\psi}{2}S\frac{\theta}{2}S\frac{\phi}{2} \\ Im_{|0\rangle} = S\frac{\psi}{2}S\frac{\theta}{2}C\frac{\phi}{2} - C\frac{\psi}{2}C\frac{\theta}{2}S\frac{\phi}{2} \\ Re_{|1\rangle} = C\frac{\psi}{2}S\frac{\theta}{2}C\frac{\phi}{2} + S\frac{\psi}{2}C\frac{\theta}{2}S\frac{\phi}{2} \\ Im_{|1\rangle} = C\frac{\psi}{2}S\frac{\theta}{2}S\frac{\phi}{2} - S\frac{\psi}{2}C\frac{\theta}{2}C\frac{\phi}{2} \end{cases} \tag{30}$$

Expression (29), or the detailed version (30), appears to be the most complete way to define and express a given qubit state. They also establish the transformation from the YPR angles to the quantum computing domain. Establishing the inverse transformation implies the comparison of expressions (25) and (30). This reveals the following relationships between a quaternion and qubit state components:

$$\begin{cases} Re_{|0\rangle} = r \\ Im_{|0\rangle} = -z \\ Re_{|1\rangle} = y \\ Im_{|1\rangle} = -x \end{cases} \tag{31}$$

Relationship (31) supports and generalises the result obtained in Section 3.2. Moreover, considering relations (27) and (31), the homogenous orientation matrix can be derived directly from the qubit state's representation shown below:

$$M_{YPR}(\psi,\theta,\varphi) = R_z(\varphi)R_y(\theta)R_x(\psi)$$

$$= \begin{pmatrix} Re_{|0\rangle}{}^2 + Im_{|1\rangle}{}^2 - Re_{|1\rangle}{}^2 - Im_{|0\rangle}{}^2 & -2Im_{|1\rangle}Re_{|1\rangle} + 2Re_{|0\rangle}Im_{|0\rangle} & 2Re_{|0\rangle}Re_{|1\rangle} + 2Im_{|1\rangle}Im_{|0\rangle} \\ -2Re_{|0\rangle}Im_{|0\rangle} - 2Im_{|1\rangle}Re_{|1\rangle} & Re_{|0\rangle}{}^2 - Im_{|1\rangle}{}^2 + Re_{|1\rangle}{}^2 - Im_{|0\rangle}{}^2 & -2Re_{|1\rangle}Im_{|0\rangle} + 2Re_{|0\rangle}Im_{|1\rangle} \\ 2Im_{|1\rangle}Im_{|0\rangle} - 2Re_{|0\rangle}Re_{|1\rangle} & -2Re_{|0\rangle}Im_{|1\rangle} - 2Re_{|1\rangle}Im_{|0\rangle} & Re_{|0\rangle}{}^2 - Im_{|1\rangle}{}^2 - Re_{|1\rangle}{}^2 + Im_{|0\rangle}{}^2 \end{pmatrix} \quad (32)$$

This also establishes the calculation of the YPR angles from a given qubit state, as shown in (33).

$$\begin{cases} \psi = \frac{1}{2} Asin(2(Re_{|0\rangle}Re_{|1\rangle} - Im_{|0\rangle}Im_{|1\rangle})) \\ \theta = \frac{1}{2} Atan\,2\big(-2(Re_{|0\rangle}\,Im_{|1\rangle} + Re_{|1\rangle}Im_{|0\rangle}), 1 - 2\big(Im_{|1\rangle}{}^2 + Re_{|1\rangle}{}^2\big)\big) \\ \varphi = \frac{1}{2} Atan\,2\big(-2(Re_{|0\rangle}Im_{|0\rangle} + Re_{|1\rangle}Im_{|1\rangle}), 1 - 2\big(Re_{|1\rangle}{}^2 + Im_{|1\rangle}{}^2\big)\big) \end{cases} \quad (33)$$

## 3. Results and discussion

Based on the concepts developed and analysed above, it appears that a quaternion can be expressed using a qubit state as follows:

$$q = Re_{|0\rangle} - Im_{|1\rangle}\,i + Re_{|1\rangle}\,j - Im_{|0\rangle}\,k \quad (34)$$

Furthermore, a qubit state can be expressed using a given unit quaternion as follows:

$$|q\rangle = \begin{pmatrix} r - iz \\ y - ix \end{pmatrix} \quad (35)$$

Both expressions are valid if the initial qubit state is considered to be $|0\rangle$, which is the case in most, if not all, quantum computing circuits and algorithms conceived so far.

### 3.1. Illustrative example

The orientation of a robotic arm is simulated herein, first using the YPR angles (relation (13)), then converted to quaternions (relation (25)), then to qubit states (relation (35)), and then using a qubit state in an online quantum computing simulator [36]. The quantum spin operators are obtained from $R_x(-\varphi)R_y(\theta)R_z(-\psi)$ instead of $R_z(\varphi)R_y(\theta)R_x(\psi)$, as mentioned in Section 3.2. This yields a qubit state that matches a quaternion representation, such as $q = Re_{|0\rangle} + Im_{|0\rangle}\,i + Re_{|1\rangle}\,j + Im_{|1\rangle}\,k$.

The orientation of the end effector varies according to a fifth-order polynomial [37] with the following initial and final conditions:

$$\begin{cases} \psi = 0 \rightarrow \frac{\pi}{2} rad \\ \theta = 0 \rightarrow \frac{\pi}{4} rad \\ \phi = 0 \rightarrow \frac{\pi}{3} rad \end{cases}$$

### 3.2. Simulation results

Fig. 6 depicts the quantum circuit used to compute the qubit states corresponding to several YPR angles.

Fig. 7 shows the variations in the YPR angles, whereas Fig. 8 summarises the qubit states for each angle value computed using the online quantum simulator [36].

Fig. 9 shows the resulting qubit states computed using the online quantum simulator along with the equivalent quaternion calculations performed using Matlab software.

The results were obtained using the quantum operator $R_x(-\varphi)R_y(\theta)R_z(-\psi)$ applied to the initial qubit state $|0\rangle$. This results in a qubit state that matches the quaternion components, such that $Re_{|0\rangle} = r$, $Im_{|0\rangle} = x$, $Re_{|1\rangle} = y$, and $Im_{|1\rangle} = z$. The

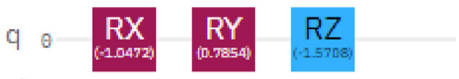


*Fig. 6. Quantum circuit with the computed final qubit states (quantum circuit realised with [36]).*

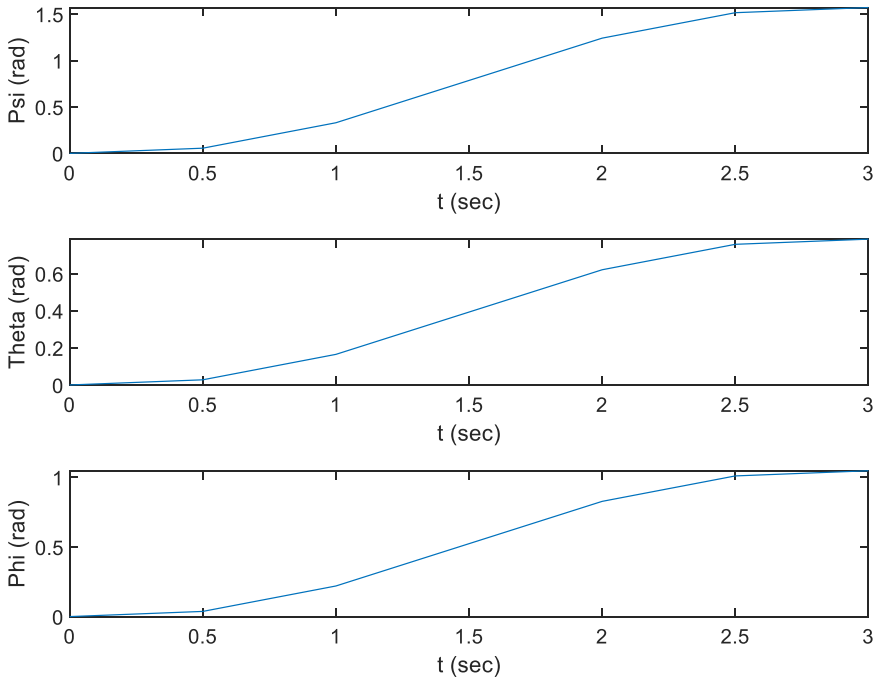


*Fig. 7. YPR angles variation.*

equivalence between the quaternions and the qubit states (Section 3.2) appears to be effective. Moreover, the YPR angles are divided by 2 in both representations because of the sandwich product of the transformations and not as a result of the developed representation of the qubit state or the angle $\varphi$ ranging in principle from 0 to $\pi$ radians. Therefore, we also multiply the angles by 2 in the simulation.

### 3.3. Further analysis

From equations (13), (27), (30) and (31), the 3D representation of the oz axis undergoing the three elementary rotations, or its final orientation represented by a vector $v$, can be expressed as shown in formula (36) using the quaternion's components, or using the qubit state's components as shown in equation (37), or using the YPR angles as shown in relationship (38).

$$v=\begin{pmatrix} 2ry+2xz \\ 2yz-2rx \\ r^2-x^2-y^2+z^2 \end{pmatrix} \tag{36}$$

$$v=\begin{pmatrix} 2Re_{|0\rangle}Re_{|1\rangle}+2Im_{|0\rangle}Im_{|1\rangle} \\ -2Im_{|0\rangle}Re_{|1\rangle}-2Re_{|0\rangle}Im_{|1\rangle} \\ {Re_{|0\rangle}}^2-{Im_{|1\rangle}}^2-{Re_{|1\rangle}}^2+{Im_{|0\rangle}}^2 \end{pmatrix} \tag{37}$$

$$v=\begin{pmatrix} C\psi S\theta C\varphi+S\psi S\varphi \\ C\psi S\theta S\varphi-S\psi C\varphi \\ C\psi C\theta \end{pmatrix} \tag{38}$$

Setting the angles $\psi=0$, $\theta=0$, and $\varphi=0$ for both the YPR angles and qubit states in the quantum computing representation developed in this article leads to the following expressions:

$$M_{YPR}(0,0,0)=\begin{pmatrix} 1 & 0 & 0 \\ 0 & 1 & 0 \\ 0 & 0 & 1 \end{pmatrix} \text{ with}$$
$$v=\begin{pmatrix} 0 \\ 0 \\ 1 \end{pmatrix} \text{ and } \begin{cases} Re_{|0\rangle}=1 \\ Im_{|0\rangle}=0 \\ Re_{|1\rangle}=0 \\ Im_{|1\rangle}=0 \end{cases} \text{ or } |q\rangle=|0\rangle \tag{39}$$

Using $\psi=0$, $\theta=\pi$, and $\varphi=0$ gives the following result:

$$M_{YPR}(0,\pi,0)=\begin{pmatrix} -1 & 0 & 0 \\ 0 & 1 & 0 \\ 0 & 0 & -1 \end{pmatrix} \text{ with}$$
$$v=\begin{pmatrix} 0 \\ 0 \\ -1 \end{pmatrix} \text{ and } \begin{cases} Re_{|0\rangle}=0 \\ Im_{|0\rangle}=0 \\ Re_{|1\rangle}=1 \\ Im_{|1\rangle}=0 \end{cases} \text{ or } |q\rangle=|1\rangle \tag{40}$$

Using $\psi=0$, $\theta=0$ and $\varphi=\pi$ gives the following result:

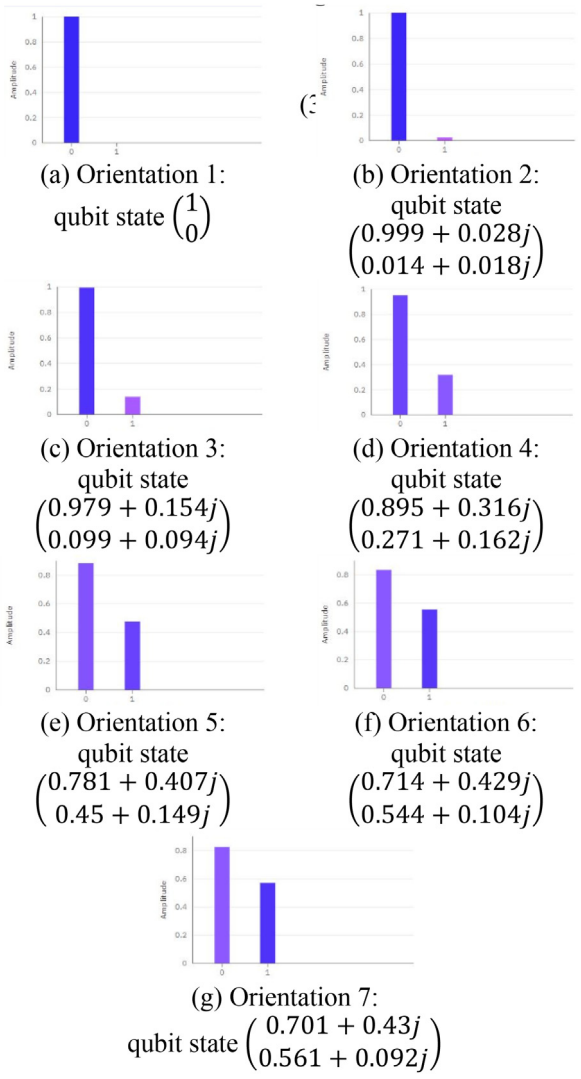


*Fig. 8. The qubit states computed for each angle range (results obtained with [36]).*

$$M_{YPR}(0,\pi,\pi)=\begin{pmatrix}1&0&0\\0&-1&0\\0&0&-1\end{pmatrix}\text{ with }$$
$$v=\begin{pmatrix}0\\0\\-1\end{pmatrix}\text{ and }\begin{cases}Re_{|0\rangle}=0\\Im_{|0\rangle}=0\\Re_{|1\rangle}=0\\Im_{|1\rangle}=1\end{cases}\text{ or }|q\rangle=i|1\rangle \tag{41}$$

It appears that the oz axis corresponds to quantum state $|0\rangle$ (39), and a rotation $\pi$ around the quantum oy axis leads to state $|1\rangle$ (40), which is in the opposite direction of the oz axis. A rotation $\pi$ around the oy axis inverts the orientation of both the ox and oz axes and leaves oy unchanged. Finally, a rotation $\pi$ around the quantum ox axis leads to state $i|1\rangle$ (41), which is also in the opposite direction of the oz axis, and a rotation $\pi$ around the ox axis inverts the sign of both orientations of the oy and oz axes and leaves the ox axis unchanged. This implies that the X gate is actually a $\pi$ rotation around the oy axis and the Y gate is actually a $\pi$ rotation around the ox axis.

Performing the same operations with half YPR angles gives the following:

$$M_{YPR}(0,0,0)=\begin{pmatrix}1&0&0\\0&1&0\\0&0&1\end{pmatrix}\text{ with}$$
$$v=\begin{pmatrix}0\\0\\1\end{pmatrix}\text{ and }\begin{cases}Re_{|0\rangle}=1\\Im_{|0\rangle}=0\\Re_{|1\rangle}=0\\Im_{|1\rangle}=0\end{cases}\text{ or }|q\rangle=|0\rangle \tag{42}$$

Using $\psi=0$, $\theta=\frac{\pi}{2}$ and $\varphi=0$ gives the following result:

$$M_{YPR}\left(0,\tfrac{\pi}{2},0\right)=\begin{pmatrix}0&0&1\\0&1&0\\-1&0&0\end{pmatrix}\text{ with }v=\begin{pmatrix}1\\0\\0\end{pmatrix}$$
$$\text{and }\begin{cases}Re_{|0\rangle}=\frac{\sqrt{2}}{2}\\Im_{|0\rangle}=0\\Re_{|1\rangle}=\frac{\sqrt{2}}{2}\\Im_{|1\rangle}=0\end{cases}\text{ or }|q\rangle=\frac{\sqrt{2}}{2}|0\rangle+\frac{\sqrt{2}}{2}|1\rangle \tag{43}$$

Using $\psi=0$, $\theta=\frac{\pi}{2}$ and $\varphi=\frac{\pi}{2}$ gives the following result:

$$M_{YPR}\left(0,\tfrac{\pi}{2},\tfrac{\pi}{2}\right)=\begin{pmatrix}0&-1&0\\0&0&1\\-1&0&0\end{pmatrix}\text{ with }v=\begin{pmatrix}0\\1\\0\end{pmatrix}$$
$$\text{and }\begin{cases}Re_{|0\rangle}=\frac{1}{2}\\Im_{|0\rangle}=-\frac{1}{2}\\Re_{|1\rangle}=\frac{1}{2}\\Im_{|1\rangle}=\frac{1}{2}\end{cases}\text{ or }|q\rangle=\left(\frac{1}{2}-\frac{1}{2}i\right)|0\rangle+\left(\frac{1}{2}+\frac{1}{2}i\right)|1\rangle \tag{44}$$

It is tempting to conclude that assuming the quantum computing angles to be twice their equivalent YPR angles leads to the same result in both representations, as relations (42), (43), and (44)

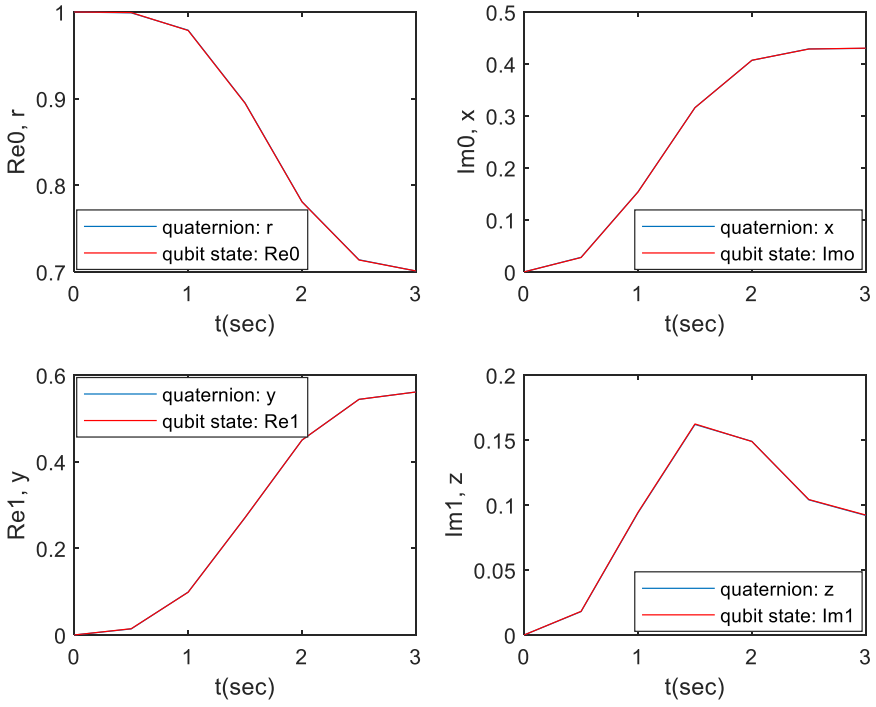


*Fig. 9. Quaternion and qubit state results for each angle range.*

imply. However, this is inconsistent with the gate reversibility. For example, applying equation (42) twice gives $v = \begin{pmatrix} 0 \\ 0 \\ -1 \end{pmatrix}$ instead of the expected result $v = \begin{pmatrix} 0 \\ 0 \\ 1 \end{pmatrix}$, whereas applying $R_y(\pi)$ twice to state $|0\rangle$ gives the same initial state $|0\rangle$, owing to the quantum gate's fundamental reversibility.

The relationship between the YPR and quantum spin representations appears to apply to half angles in the former case versus double angles in the latter case.

To summarise, a reference frame ($o_0$ $x_0$ $y_0$ $z_0$) is considered to be described in the YPR representation as shown below:

$$\begin{cases} (ox) \equiv (o_0 x_0) \\ (oy) \equiv (o_0 y_0) \\ (oz) \equiv (o_0 z_0) \end{cases} \tag{45}$$

The axes are therefore described as follows in the spherical representation:

$$\begin{cases} (ox) \equiv (o_0 z_0) \\ (oy) \equiv (o_0 x_0) \\ (oz) \equiv (o_0 y_0) \end{cases} \tag{46}$$

The axes are described as follows in the quaternion's representation:

$$\begin{cases} (ox) \equiv -(o_0 z_0) \\ (oy) \equiv (o_0 y_0) \\ (oz) \equiv -(o_0 x_0) \end{cases} \tag{47}$$

The axes are described as follows in the quantum computing-based representation:

$$\begin{cases} (ox) \equiv (o_0 x_0), considering\ 2\psi \\ (oy) \equiv (o_0 y_0), considering\ 2\theta \\ (oz) \equiv (o_0 z_0), considering\ 2\varphi \end{cases} \tag{48}$$

Moreover, the quantum states corresponding to the three axes should be obtainable using a systematic approach, for instance, based on the basic rotations. Representing the three unit vectors of the ox, oy, and oz axes ($u_x$, $u_y$ and $u_z$) using their quantum qubit states $\begin{pmatrix} \alpha_x \\ \beta_x \end{pmatrix}$, $\begin{pmatrix} \alpha_y \\ \beta_y \end{pmatrix}$, and $\begin{pmatrix} \alpha_z \\ \beta_z \end{pmatrix}$, a $\frac{\pi}{2}$ rotation ($\pi$ in quantum computing) around the ox axis on the qubit state $\begin{pmatrix} \alpha_y \\ \beta_y \end{pmatrix}$ should result in the oz axis or qubit state $\begin{pmatrix} \alpha_z \\ \beta_z \end{pmatrix}$. The same rotation around the oy axis on the qubit state $\begin{pmatrix} \alpha_z \\ \beta_z \end{pmatrix}$ should result in the ox axis or qubit state $\begin{pmatrix} \alpha_x \\ \beta_x \end{pmatrix}$, and likewise around

the oz axis on the qubit state $\begin{pmatrix}\alpha_x\\ \beta_x\end{pmatrix}$ should result in the oy axis or qubit state $\begin{pmatrix}\alpha_y\\ \beta_y\end{pmatrix}$. This can be expressed in the three relationships shown below:

$$\begin{pmatrix}0 & -i\\ -i & 0\end{pmatrix}\begin{pmatrix}\alpha_y\\ \beta_y\end{pmatrix}=\begin{pmatrix}\alpha_z\\ \beta_z\end{pmatrix} \tag{49}$$

$$\begin{pmatrix}0 & -1\\ 1 & 0\end{pmatrix}\begin{pmatrix}\alpha_z\\ \beta_z\end{pmatrix}=\begin{pmatrix}\alpha_x\\ \beta_x\end{pmatrix} \tag{50}$$

$$\begin{pmatrix}-i & 0\\ 0 & i\end{pmatrix}\begin{pmatrix}\alpha_x\\ \beta_x\end{pmatrix}=\begin{pmatrix}\alpha_y\\ \beta_y\end{pmatrix} \tag{51}$$

These expressions lead to the following system under the condition $|\alpha_x|^2+|\beta_x|^2=|\alpha_y|^2+|\beta_y|^2=|\alpha_z|^2+|\beta_z|^2=1$:

$$\begin{cases}-i\beta_y=\alpha_z\\ -i\alpha_y=\beta_z\\ -\beta_z=\alpha_x\\ \alpha_z=\beta_x\\ -i\alpha_x=\alpha_y\\ i\beta_x=\beta_y\end{cases} \tag{52}$$

An infinite number of possible solutions exist for system (52). One of these solutions considers the qubit state $\begin{pmatrix}\alpha_z\\ \beta_z\end{pmatrix}$ as $|0\rangle$, with $\alpha_z=1$ and $\beta_z=0$. The remaining qubit state $\begin{pmatrix}\alpha_x\\ \beta_x\end{pmatrix}$ can then be considered as $|1\rangle$ with $\alpha_x=0$ and $\beta_x=1$, and the state $\begin{pmatrix}\alpha_y\\ \beta_y\end{pmatrix}$ as $i|1\rangle$ with $\alpha_y=0$ and $\beta_y=i$. The oz, ox, and oy axes thus appear to correspond to states $|0\rangle$, $|1\rangle$, and $i|1\rangle$, respectively.

Other possible solutions lead to the same qubit states but with permutations. That is, for instance, the states $\begin{pmatrix}\alpha_z\\ \beta_z\end{pmatrix}$, $\begin{pmatrix}\alpha_y\\ \beta_y\end{pmatrix}$, and $\begin{pmatrix}\alpha_x\\ \beta_x\end{pmatrix}$ become $|1\rangle$, $i|1\rangle$, and $|0\rangle$, respectively.

A more convenient and realistic representation of the qubit state and the quantum eigenstates can be illustrated, as shown in Fig. 10.

### 3.4. Validation of the proposed representation

To validate the proposed representation, the ox, oy, and oz axes, corresponding respectively to the states $|1\rangle$, $i|1\rangle$, and $|0\rangle$, are rotated over an arc spanning $\pi$ radians, equivalent to $\frac{\pi}{2}$ in the 3D vector space. A $\pi$ rotation of the oz axis around the ox axis should lead successively to $-$oy, $-$oz, and then oy. A similar rotation of the ox axis around oy should lead to $-$oz, $-$ox, and then oz. Similarly, rotating the oy axis around oz over $\pi$ radians should lead to $-$ox, $-$oy, and then ox. These transitions are indicated in the matrix relations expressed below.

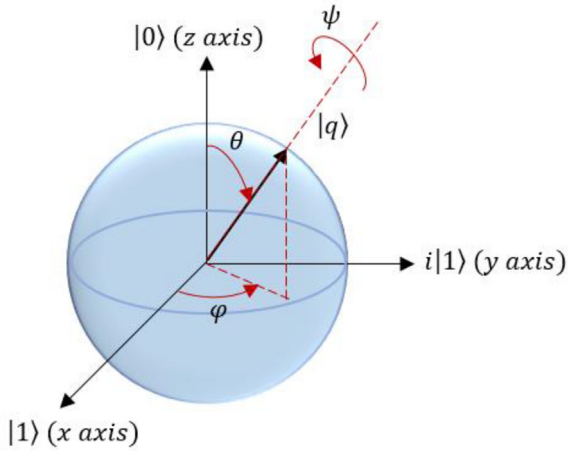


*Fig. 10. Proposed comprehensive representation of a qubit state.*

$$\begin{pmatrix}0 & -i\\ -i & 0\end{pmatrix}\begin{pmatrix}1\\ 0\end{pmatrix}=\begin{pmatrix}0\\ -i\end{pmatrix} \tag{53.a}$$

$$\begin{pmatrix}0 & -i\\ -i & 0\end{pmatrix}\begin{pmatrix}0\\ -1\end{pmatrix}=\begin{pmatrix}-1\\ 0\end{pmatrix} \tag{53.b}$$

$$\begin{pmatrix}0 & -i\\ -i & 0\end{pmatrix}\begin{pmatrix}-1\\ 0\end{pmatrix}=\begin{pmatrix}0\\ i\end{pmatrix} \tag{53.c}$$

$$\begin{pmatrix}0 & -1\\ 1 & 0\end{pmatrix}\begin{pmatrix}0\\ 1\end{pmatrix}=\begin{pmatrix}-1\\ 0\end{pmatrix} \tag{54.a}$$

$$\begin{pmatrix}0 & -1\\ 1 & 0\end{pmatrix}\begin{pmatrix}-1\\ 0\end{pmatrix}=\begin{pmatrix}0\\ -1\end{pmatrix} \tag{54.b}$$

$$\begin{pmatrix}0 & -1\\ 1 & 0\end{pmatrix}\begin{pmatrix}0\\ -1\end{pmatrix}=\begin{pmatrix}1\\ 0\end{pmatrix} \tag{54.c}$$

$$\begin{pmatrix}-i & 0\\ 0 & i\end{pmatrix}\begin{pmatrix}0\\ i\end{pmatrix}=\begin{pmatrix}0\\ -1\end{pmatrix} \tag{55.a}$$

$$\begin{pmatrix}-i & 0\\ 0 & i\end{pmatrix}\begin{pmatrix}0\\ -1\end{pmatrix}=\begin{pmatrix}0\\ -i\end{pmatrix} \tag{55.b}$$

$$\begin{pmatrix}-i & 0\\ 0 & i\end{pmatrix}\begin{pmatrix}0\\ -i\end{pmatrix}=\begin{pmatrix}0\\ 1\end{pmatrix} \tag{55.c}$$

## 4. Conclusion

This article presents an original and comprehensive analysis of several mathematical tools used to define the spatial rotation of rigid bodies and examines their equivalences in the context of quantum spins as an effective model for describing object orientations.

The development of the proposed quantum representation of a qubit state raises a few conceptual problems, such as the linear interdependency of the two eigenvectors, incomplete information on the spin of a qubit around itself, and the proper definition of the 2D quantum vector representation in terms of the classical 3D axes.

The proposed work addresses three major issues and proposes solutions to them. First, regarding the lack of information in the current Bloch representation of a qubit state in reference to the self-spin angle (around the oz axis), a comprehensive representation that contains the roll rotation, which is required in various practical applications, is proposed.

Second, regarding the essential specification of the 3D axes that do not correspond to the existing representation, the current depiction uses half angles and assumes aligned ox and oz axes, which contradicts the rational and widely accepted 3D representation. The proposed representation addresses this by including a proper characterisation of the three fundamental spatial axes.

Third, the ratio of the oy axis rotation angle must be considered, not only for sandwich products but also to accurately represent the genuine rotation angles in 3D space.

Several equivalences are found to exist between the different representations of rotation and quantum spins. The new comprehensive and more intuitive way of representing a qubit state may help guide future studies aimed at modelling orientation-based processes using a single qubit state for various applications in quantum computing, such as industrial robots, autonomous vehicles, and aircraft.

### Conflicts of interest

The authors declare that they have no known competing financial interests or personal relationships that could have appeared to influence the work reported in this paper.

## Acknowledgement

The authors would like to warmly thank École Nationale Polytechnique of Algiers for all the resources and discussions that led to the conclusions of this report.

## References

[1] K. Nagata, T. Nakamura, Quantum algorithm for the root-finding problem, Quant. Stud. Math. Found. 6 (2019) 135–139, https://doi.org/10.1007/s40509-018-0171-0.
[2] T. Xin, S. Wei, J. Cui, J. Xiao, I. Arrazola, L. Lamata, X. Kong, D. Lu, E. Solano, G. Long, A quantum algorithm for solving linear differential equations: theory and experiment, Phys. Rev. 101 (2020) 32307–32318, https://doi.org/10.1103/PhysRevA.101.032307.
[3] R.H. Preston, Applying grover's algorithm to hash functions: a software perspective, IEEE Transac. Quant. Eng. 3 (2023) 2500710–2500719, https://doi.org/10.1109/TQE.2022.3233526.
[4] M.Z. Sarikaya, N. Alp, Q-laplace transform on quantum integral, 2023, pp. 153–164, https://doi.org/10.46793/KgJMat2301.153A, 47.
[5] L. Wossnig, Z. Zhao, A. Prakash, A quantum linear system algorithm for dense matrices, Phys. Rev. Lett. 120 (2018) 50502–50507, https://doi.org/10.1103/PhysRevLett.120.050502.
[6] O. Kyriienko, Quantum inverse iteration algorithm for programmable quantum simulators, npj Quant. Info. 6 (2020) 1–8, https://doi.org/10.1038/s41534-019-0239-7.
[7] Y. Mahmoudi, N. Zioui, H. Belbachir, M. Tadjine, A. Rezgui, A brief review on mathematical tools applicable to quantum computing for modelling and optimization problems in engineering, Emerg. Sci. J. 7 (2023) 289–312, https://doi.org/10.28991/ESJ-2023-07-01-020.
[8] N. Zioui, Y. Mahmoudi, A. Mahmoudi, M. Tadjine, S. Bentouba, A new quantum computing based algorithm for robotic arms and rigid bodies' orientation, J. Appl. Comput. Mech. 7 (2021) 1836–1846, https://doi.org/10.22055/JACM.2021.37611.3048.
[9] M. Fazilat, N. Zioui, J. St-Arnaud, A novel quantum model of forward kinematics based on quaternion/Pauli gate equivalence: application to a six-jointed industrial robotic arm, Res. Eng. 14 (2022) 100402–100410, https://doi.org/10.1016/j.rineng.2022.100402. Elsevier.
[10] A. Benghezal, A. Nemra, Bouaziz Ni, M. Tadjine, New robust backstepping attitude control approach applied to quanser 3 DOF hover quadrotor in the case of actuators faults, Unmanned. Syst. 11 (2022) 1–15, https://doi.org/10.1142/S2301385024500018.
[11] K. Eliker, S. Grouni, M. Tadjine, W. Zhang, Quadcopter nonsingular finite-time adaptive robust saturated command-filtered control system under the presence of uncertainties and input saturation, Nonlinear Dynam. 104 (2021) 1363–1387, https://doi.org/10.1007/s11071-021-06332-3.
[12] A. Allam, A. Nemra, M. Tadjine, Parametric and implicit features-based UAV–UGVs time-varying formation tracking: dynamic approach, Unmanned Syst. 10 (2022) 109–128, https://doi.org/10.1142/S2301385022500066.
[13] K. Eliker, S. Grouni, M. Tadjine, W. Zhang, Practical finite time adaptive robust flight control system for quad-copter UAVs, Aero. Sci. Technol. 98 (2020) 105708–105728, https://doi.org/10.1016/j.ast.2020.105708.
[14] Y. Saidi, A. Nemra, M. Tadjine, Robust mobile robot navigation using fuzzy type 2 with wheel slip dynamic modeling and parameters uncertainties, Int. J. Model Simulat. 40 (2020) 397–420, https://doi.org/10.1080/02286203.2019.1646480.
[15] A. Rezoug, J. Iqbal, M. Tadjine, Extended grey wolf optimization–based adaptive fast nonsingular terminal sliding mode control of a robotic manipulator, Proc. IME J. Syst. Control. Eng. 236 (2022) 1738–1754, https://doi.org/10.1177/09596518221099.
[16] N. Zioui, A. Mahmoudi, Y. Mahmoudi, M. Tadjine, Quantum computing based state domain equations and feedback control, Res. Appl. Math. 19 (2023) 100385–100393, https://doi.org/10.1016/j.rinam.2023.100385.
[17] D. McMahon, Quantum Computing Explained, first ed., Wiley - IEEE, New Jersey. 2008 https://doi.org/10.1002/9780470181386.

[18] J. Abhijith, A. Adedoyin, J. Ambrosiano, P. Anisimov, W. Casper, G. Chennupati, C. Coffrin, H. Djidjev, D. Gunter, S. Karra, N. Lemons, S. Lin, A. Malyzhenkov, D. Mascarenas, S. Mniszewski, B. Nadiga, D. O'Malley, D. Oyen, S. Pakin, L. Prasad, R. Roberts, P. Romero, N. Santhi, N. Sinitsyn, P.J. Swart, J.G. Wendelberger, B. Yoon, R. Zamora, W. Zhu, S. Eidenbenz, A. Bärtschi, P.J. Coles, M. Vuffray, A.Y. Lokhov, Quantum algorithm implementations for beginners, ACM Transac. Quant. Comput. 3 (2022) 1–92, https://doi.org/10.1145/3517340.

[19] D. Aerts, M.S. de Bianchi, The Extended Bloch Representation of Quantum Mechanics and the Hidden-Measurement Solution to the Measurement Problem, vol. 351, 2014, pp. 975–1025, https://doi.org/10.1016/j.aop.2014.09.020.

[20] S. Heusler, P. Schlummer, M.S. Ubben, A knot theoretic extension of the Bloch sphere representation for qubits in hilbert space and its application to contextuality and many-worlds theories, Symmetry 12 (2020) 1135–1158, https://doi.org/10.3390/sym12071135.

[21] M.E.A. Boudjoghra, S.A.S. Daimellah, N. Zioui, Y. Mahmoudi, M. Tadjine1, State-Domain equations and their quantum computing solution based HHL algorithm, Math. Modell. Eng. Probl. 9 (2022) 879–886, https://doi.org/10.18280/mmep.090404.

[22] L. Santelli, P. Orlandi, R. Verzicco, A finite–difference scheme for three–dimensional incompressible flows in spherical coordinates, J. Comput. Phys. 424 (2021) 109848–109864, https://doi.org/10.1016/j.jcp.2020.109848.

[23] C. Martin, A. Petrusel, Free surface equatorial flows in spherical coordinates with discontinuous stratification depending on depth and latitude, Ann. Mat. Pura. Appl. 201 (2022) 2677–2690, https://doi.org/10.1007/s10231-022-01214-w.

[24] A. Crnkić, Z. Kapić, Interpolation on the special orthogonal group with highdimensional Kuramoto model, IOP Conf. Ser. Mater. Sci. Eng. 1208 (2021) 12037–12043, https://doi.org/10.1088/1757-899X/1208/1/012037.

[25] H.-Y. Lin, M. Cahay, B.N. Vellambi, D. Morris, A generalization of quaternions and their application, Symmetry 14 (2022) 599–625, https://doi.org/10.3390/sym14030599.

[26] T. Bajd, M. Mihelj, M. Munih, Introduction to Robotics, first ed., Springer Dordrecht Heidelberg, New York, London. 2013 https://doi.org/10.1007/978-94-007-6101-8.

[27] M. Ceccarelli, eds., Robot Manipulators, Intech, Croatia. 2008, https://doi.org/10.5772/87.

[28] A. Al Attar, P. Kormushev, Kinematic-model-free orientation control for robot manipulation using locally weighted dual quaternions, Robotics 9 (2020) 76–88, https://doi.org/10.3390/robotics9040076.

[29] F. Frigeni, Industrial Robotics Control Mathematical Models, Software Architecture, and Electronics Design, Apress, first ed., Springer Science & Business Media, New York. 2023 https://doi.org/10.1007/978-1-4842-8989-1.

[30] L. Chen, T. Zielinska, J. Wang, W. Ge, Solution of an inverse kinematics problem using dual quaternions, Int. J. Appl. Math. Comput. Sci. 30 (2020) 351–361, https://doi.org/10.34768/amcs-2020-0027.

[31] A. Valverde, P. Tsiotras, Spacecraft robot kinematics using dual quaternions, Robotics 7 (2018) 64–87, https://doi.org/10.3390/robotics7040064.

[32] I. Mas, C. Kitts, Quaternions and dual quaternions: singularity-free multirobot formation control, J. Intell. Rob. Syst. 87 (2016) 643–660, https://doi.org/10.1007/s10846-016-0445-x.

[33] A.J. Hanson, Visualizing Quaternions, first ed., Morgan Kaufmann Series in Interactive 3D Technology, San Francisco, CA. 2006 https://doi.org/10.1145/1198555.1198701.

[34] Y. Li, G. Fu, Quaternion-based conversion formulas for kinematic attitude of floating offshore wind turbines (FOWT), IOP Conf. Ser. Mater. Sci. Eng. 301 (2018) 12094–12099, https://doi.org/10.1088/1757-899X/301/1/012094.

[35] S. Sarabandi, F. Thomas, Accurate computation of quaternions from rotation matrices, Adv. Robot Kinem. (2019) 39–46, https://doi.org/10.1007/978-3-319-93188-3_5. Chapter 5.

[36] IBM Quantum Composer. https://quantum-computing.ibm.com/composer/files/new (accessed March 8, 2023).

[37] P.A. Parikh, R.R. Trivedi, K.D. Joshi, Trajectory planning of a 5 DOF feeding serial manipulator using 6 th order polynomial method, J. Phys. Conf. 1921 (2021) 12088–12105, https://doi.org/10.1088/1742-6596/1921/1/012088.